Pharmacogn J. 2023; 15(2): 266-278
A Multifaceted Journal in the field of Natural Products and Pharmacognosy
www.phcogj.com

Original Article

Development and Evaluation of Bio fabricated Silver Nanoparticles from *Blumea lacera* for *In-vitro* Antibacterial, Antioxidant and Anti-inflammatory Activity

Tarkeshwar Dubey[1], Kancharla Bhanukiran[1], Kuna Das[2], Siva Hemalatha[1,*]

Tarkeshwar Dubey[1], Kancharla Bhanukiran[1], Kuna Das[2], Siva Hemalatha[1,*]

[1]*Department of Pharmaceutical Engineering & Technology, Indian Institute of Technology, Banaras Hindu University, Varanasi-221005, INDIA.*

[2]*Department of Biotechnology and Medical Engineering, National Institute of Technology, Rourkela, Odisha-769008, INDIA.*

Correspondence

Siva Hemalatha

Department of Pharmaceutical Engineering & Technology, Indian Institute of Technology, Banaras Hindu University, Varanasi-221005, INDIA.

E-mail: shemalatha.phe@itbhu.ac.in

History

- Submission Date: 17-12-2022;
- Review completed: 02-02-2023;
- Accepted Date: 13-02-2023.

DOI : 10.5530/pj.2023.15.38

Article Available online

http://www.phcogj.com/v15/i6

ABSTRACT

Background: Increasing prevalence of microbial resistance and side effects of currently available drugs compels the researchers to look for alternate therapies and formulations to overcome this problem. Plant based formulations have been proved to be most reliable agents in recent times. **Objective:** In the current study, bio fabricated herbal silver nanoparticles (HSNPs) were prepared by reducing silver nitrate ($AgNO_3$) solution with ethyl acetate fractions (EAF) of *Blumea lacera* extracts. These bios conjugated HSNPs were then assessed for potential anti-inflammatory and antibacterial activities along with *in vitro* antioxidant effect. **Methods and results:** The synthesis was confirmed by absorbance peak at 441 nm due to surface plasmon resonance in UV-visible spectrophotometer. FTIR spectra of HSNPs indicated the phytochemicals having C-O bond responsible for reducing of Ag^+ to Ag^o. Average size of HSNPs was found to be 59.21 nm which was in good agreement with TEM and SEM results. EDS analysis showed the existence of Silver, Nitrogen and Carbon in HSNPs. The antibacterial activity of HSNPs in terms of zone of inhibition (ZOI) *via* disc diffusion assay and against *Staphylococcus aureus* and *Escherichia coli* was found to be 25.0±1.19 mm and 18.3±2.08 mm, respectively. The minimum inhibitory concentration (MIC) of HSNPs was found to be 50 µg/ml and 60 µg/ml against *S. aureus* and *E. coli*, respectively. The antioxidant capacity of the HSNPs was insignificant as compared to EAF but the results of anti-inflammatory activity was significant ($p<0.05$). **Conclusion:** The overall result demonstrated better *in-vitro* pharmacological potential of HSNPs compared to neat extract/EAF.

Key words: Green synthesis, Phytopharmaceuticals, Inflammation, Kukrounda, HPTLC.

INTRODUCTION

Nanoparticles, with improved properties as size, distribution, and reactivity, provide greater mechanical strength than in bulk materials. They have higher surface to volume ratio, which is mostly used for drug loading and functionalization of drug molecules.[1] Silver nanoparticles are one of the most exploited metal nanoparticles in the commercial and pharmaceutical industry because of its wide range of biomedical applicability viz. for enhancing the bioavailability of drug of interest, for sustained release formulations or for targeting the core drug moiety to the specific tissue or protein for greater efficacy.[2] In pharmaceutical industry, several chemical and physical methods are available for synthesizing nanoparticles using top-down approach or bottom-up approach.[3] Although, being used widely, these methods suffer certain limitations such as decreased biocompatibility, tedious and time taking procedure, multi-step scale-up, as well as usage of chemicals which may be toxic to humans.[4] Green synthesis approach for bio-fabrication of nanoparticles is a better alternative to overcome the aforesaid limitations and is one of most acceptable method for synthesis of nanoparticles.[5] Green technology facilitates nanoparticles synthesis by single step-one pot method involving $AgNO_3$ and a biological reducing agent[6] which may be bacteria, virus, fungi, plants or any parts of biological materials[7,8] but using plants are safe, economic, ecofriendly and easy to scale up for large production.[9,10] The biosynthesized nanoparticless involving plants, possess better activity than other biological means due to coating of secondary metabolites on NPs surface and sometimes entrapment in the metal core.[5,11] When mixed in a particular ratio with $AgNO_3$ solution, whole plant extracts possess less amount of phytoconstituents as compared to enriched fractions, which may affect the size, shape and yield of NPs.[12] Hence, fractions enriched in secondary metabolites may have better results in NPs biosynthesis. *Blumea lacera* is an annual herb with a strong odor, distributed throughout the plains of northwest India, up to an altitude of 2,000 meter.[13] This plant possesses several medicinal and therapeutic benefits.[14] The aqueous extract of the plant leaves is reported to have antifungal activity[15] antimicrobial activity[16] and wound healing activities.[17] Although, the plant is reported to have many significant pharmacological activities but remain unexplored. The plant has been used traditionally for the treatment of fever[18], cuts & bleeding wounds,[19,20] diarrhoea and other GI disorders,[21-23] piles[24-26] and also as anti-inflammatory agent.[27] Several phytoconstituents have been reported from *Blumea lacera,* especially essential oils like geneol, fenchone, coniferyl alcohol derivatives along with campesterol, flavonoids lupeol, hentriacontane, hentriacontanol, alpha-amyrin, beta-sitosterol.[28] Apart from this, a few glycosides and flavonoids have been isolated from *Blumea lacera.*[29,30] Phytosterols, such as sitosterol and campesterol present in *Blumea lacera* are reported to have potent anti-inflammatory agents.[31-34]

Cite this article: Dubey T, Bhanukiran K, Das K, Hemalatha S. Development and Evaluation of Bio fabricated Silver Nanoparticles from *Blumea lacera* for *In-vitro* Antibacterial, Antioxidant and Anti-inflammatory Activity. Pharmacogn J. 2023;15(2): 266-278.

In the current work, herbal silver nanoparticles (HSNPs) were synthesized by reduction of silver ion (Ag^+) present in silver nitrate ($AgNO_3$) solution using the ethyl acetate fractions (EAF) of *Blumea lacera* leaves extract (EBL) and explored its various pharmacological activities and compared with the neat crude extract (Figure 1).

MATERIALS AND METHODS

Materials

Silver nitrate was procured from Himedia laboaratories pvt. Ltd. (Mumbai, India), Bovine albumin was obtained from SD Fine Chemical Ltd. (Mumbai, India), standard campesterol was procured from KV Bioscientific (Lucknow, India). All the other chemicals and solvents were of AR grade. Double distilled water was utilised throughout the experimental work.

Collection and authentication of plant material

Blumea lacera leaves (collected from local area of Varanasi in Uttar Pradesh, India) were authenticated by Prof. N. K. Dubey, Department of Botany, Banaras Hindu University. A voucher specimen No. Aster. 2016/3 was deposited in the herbarium of the Institute.

Extract preparation and fractionation

The dried leaves of *Blumea lacera* plant were crushed into powder and then 100g of crushed powder was weighed and subjected for hydroalcoholic maceration (solute: solvent ratio; 1:3) for three consecutive days and the material was filtered after every day without pressing the marc except last day. After the extraction was complete, all the filtrate obtained were mixed and concentrated in rotary evaporator at 70°C and 65 RPM. The concentrated and dried extract (EBL) was fractionated through successive solvent fractionation technique using different solvents in increasing order of polarity. Five different fractions viz. hexane fraction (HF), ethyl acetate fraction (EAF), dichloromethane fraction (DCMF), butanol fraction (BuOHF) and aqueous fraction (AF) were prepared and stored until further analysis.

Standardization of fractions from EBL and quantification of campesterol in EAF

The marker-based standardization was carried out to standardize EBL and its fractions with respect to campesterol by High Performance Thin Layer Chromatography (HPTLC)-based densitometric method. Different volumes (2 to 8 µl) of standard solutions (0.05 mg/ml) and sample solution (2 and 5 µL in methanol), were applied as a band on HPTLC silica gel $60F_{254}$ aluminium plates (20×10 cm). The bands (8 mm wide) were applied at 8 mm on Y-axis and 20 mm on X-axis of the HPTLC plate by Linomat applicator (CAMAG Scientific, Switzerland). The plates were then kept for development in the pre-saturated (20 min) twin-trough chamber. using. The mobile phase used was hexane: chloroform: ethyl acetate (in a ratio 7:2:1 v/v) as mobile phase. The solvent front position was 70 mm at 25±2 °C and RH 40%. The plates were dried on a TLC plate heater (CAMAG Scientific, Switzerland) at 60°C for 5 min after development. The plates were then dipped in derivatizing chamber filled with freshly prepared p-anisaldehyde–sulfuric acid (derivatizing reagent). After dipping, the plates were again dried on a TLC plate heater at 110°C for 10 min. After derivatization, different coloured bands appeared indicating the marker compounds. These bands were then scanned at different wavelengths using TLC Scanner 4 (CAMAG Scientific, Switzerland). The amount of campesterol present in samples was quantified using linear regression equation with the help of Vision CATS software by CAMAG Scientific, Switzerland.

Synthesis of silver nanoparticles (HSNPs)

After preliminary process optimization,[35] 680 mg of silver nitrate was dissolved in 800 ml of deionised water in a 1 litre flask. To this, 200 ml of EAF (0.1 mg/ml in water) was added and adjusted the pH to 6.5. The mixture was incubated at 60°C for 3 hours followed by overnight reaction at room temperature. The effective synthesis of HSNPs was verified from the change in colour from pale yellow to reddish brown colour. The biosynthesized HSNPs were purified by centrifuging at

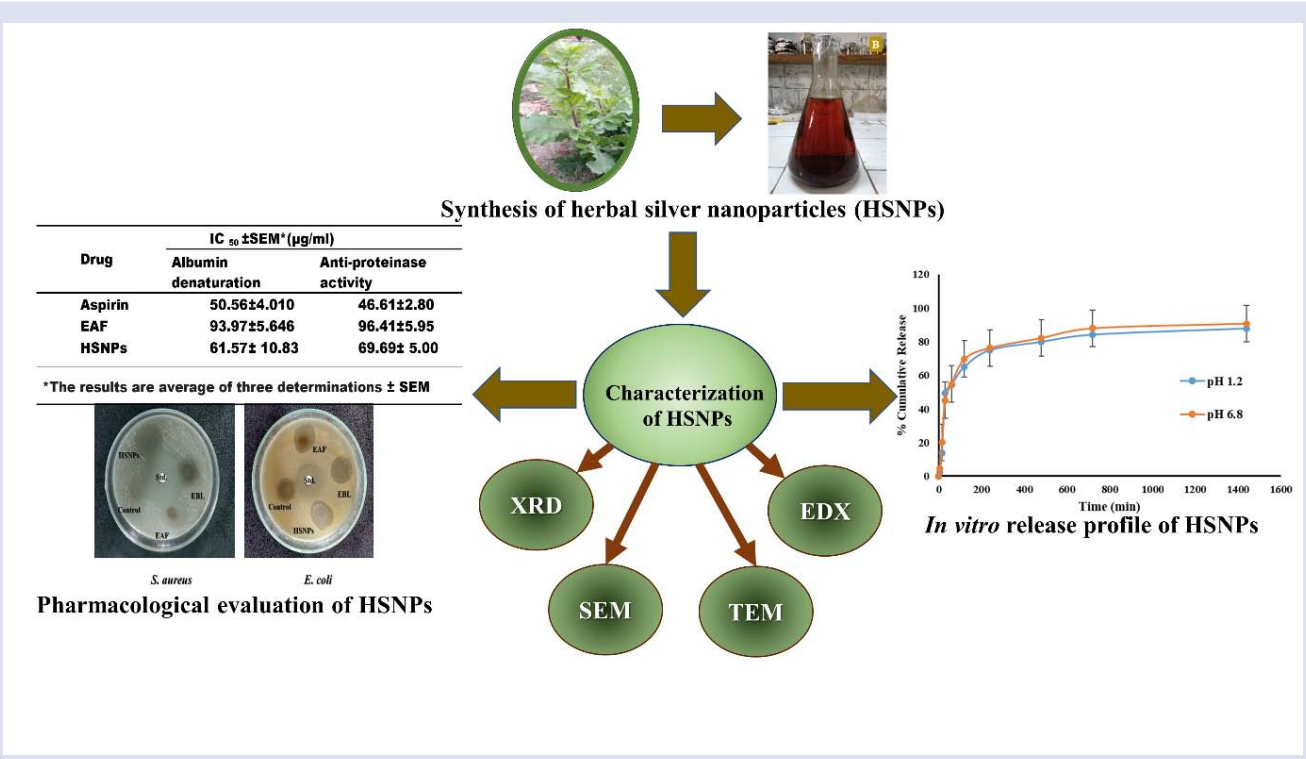

Figure 1: Synthesis, characterization, *in vitro* release, and pharmacological activity of HSNPs.

10,000 rpm for 20 minutes. Supernatant was discarded, the remaining ions and impurities from the HSNPs were separated by resuspending in deionized water and again centrifuging at 10,000 rpm for 10 minutes. The pelleted HSNPs was transferred onto a previously weighed glass petri plate and freeze dried in lyophilizer (FreeZone 1, Labconco, USA). After the removal of water, dried HSNPs were weighed and stored until further analysis.

Characterization of HSNPs

UV-visible (UV-Vis) spectrophotometric analysis

The green synthesized HSNPs colloidal solution was characterized using UV-vis spectrophotometer (Shimadzu, Japan) over the wavelength range of 200-600nm using deionized water as blank. The absorption spectrum and maximum absorption wavelength were recorded for HSNPs and $AgNO_3$ solution.

Attenuated Total Reflectance-Fourier Transform Infrared spectroscopy (ATR-FTIR analysis)

The ATR-FTIR was performed to identify the functional groups present in phytochemicals responsible for the synthesis as well as capping and stabilizing the synthesized HSNPs. HSNPs and plant extracts were spread uniformly on ATR crystal and the molecular vibrational spectra were recorded over the wavelength of $4000cm^{-1}$-$400cm^{-1}$.

Morphological analysis

Morphological analysis of HSNPs was carried out by TEM, SEM. The hydrodynamic particle size (Zavg), size distribution, and polydispersity index (PDI) of HSNPs were examined by particle size analyser (Malvern Zeta particle size analyzer, Nano ZS-90) at 25°c. Briefly, the HSNPs was diluted 10 times with ultrapure water, filtered through 0.45 µm syringe filter and analyzed by particle size analyser. The morphological evalyations were carried out by TEM and SEM analysis. The size and shape of individual HSNPs were determined by TEM (Tecnai G2 20 TWIN, FEI, USA) operated at 200 KV. Diluted HSNPs solution (10 µl) were poured on the 3 mm diameter of carbon coated Cu grid and allowed to dry overnight at 40°C. Then the size and shape of HSNPs were observed under TEM. The nature of synthesized particles (Crystalline or Amorphous) was determined by the Selected Area Electron Diffraction (SAED) Pattern. Three-dimensional shape of HSNPs was examined under SEM (Carl Zeiss Microscopy Ltd., USA) operating at 20KV. Diluted solution (20 µl) of HSNPs was spread on a clean transparent glass side and was kept in hot air oven for drying. The particles on slide were gold coated of 10nm thickness using Desk Sputter Coater machine (DSR 1, Nanostructured Coating Co., Iran). Furthermore, the morphology of HSNPs were observed in SEM with different magnification. Then, the elemental composition of HSNPs was determined using EDS analysis.

X-ray diffraction (XRD) analysis

The phase composition of HSNPs was determined by X-ray diffraction (XRD) method using X-ray diffractometer (Rigaku miniflex 600, Japan). Firstly, HSNPs solution was poured upon a silicon base followed by drying at ambient temperature. Then, the XRD diffractogram was recorded from 2θ ranging from 20 to 80° at 0.02°/minute with 2s constant time.

Quantitative estimation of various classes of phytoconstituents

All the five fractions from EBL and the synthesised HSNPs were estimated for total phenol, flavonoid and flavonol content. Total phenolic content was determined by Folin-coicalteau (FC) calorimetric method with a few modifications in which gallic acid served as a standard compound.[36] Total flavonoid and flavonol content were determined using rutin as a standard compound.[37] All the tests were performed in triplicates.

Estimation of entrapment efficiency (EE) and drug loading capacity (DLC)

HSNPs (1 g) were separated from its colloidal solution by cooling centrifugation (C-24 plus, REMI, India) at 10,000 rpm and –4°C for 20 minutes. Separated HSNPs were diluted up to 10 ml in methanol and sonicated for 1 hour to obtain a clear solution. The amount of campesterol entrapped was determined by spectrophotometric method at 210 nm (Agilent UV spectrophotometer). Methanol served as blank in this process. The %EE and %DLC of HSNPs was calculated as follows:

$$\%\ E.E = \frac{Amount\ of\ campesterol\ entrapped}{Total\ amount\ of\ campesterol} \times 100$$

$$\%\ D.L.C = \frac{Amount\ of\ campesterol\ in\ the\ HSNPs - Amount\ of\ campesterol\ in\ the\ supernatant}{Tweight\ of\ HSNPs} \times 100$$

In vitro release profile of HSNPs

For *in vitro* release study, dialysis bag method was adopted, and the study was carried out in both, simulated gastric (SGF, pH 1.2) and intestinal (SIF, pH 6.8) fluids. The release pattern of campesterol from HSNPs was determined using cellulose membrane (MWCO: 12,000–14,000). The membranes were immerged for 12 hours in the release medium prior to use. Thereafter, HSNPs (10 mg in 1 ml SGF or SIF) were filled in two dialysis bags respectively and hermetically sealed at both ends to avoid any leakage. Thereafter, both the dialysis bags were dipped into two separate 50 ml beakers filled with 40 ml SGF and SIF respectively. Both the beakers were placed and stirred at 100 rpm on magnetic stirrer while the temperature was kept constant (37±0.5°C) throughout the study (48 hrs). At specific time intervals, 5 ml sample aliquots were withdrawn and replaced by fresh buffer for maintaining sink conditions. The collected samples were analysed for campesterol content at 206 nm. To avoid any interference, blank (only SGF or SIF) was treated in the same manner.

Pharmacological screening

In vitro antioxidant activity

The study dealt with total antioxidant capacity, DPPH radical scavenging activity, alkaline dimethyl sulfoxide (DSMO) method for scavenging of the superoxide radical and the hydrogen peroxide scavenging activity.

Total antioxidant assay

Phosphomolybdenum method described by Prieto *et al.*[38] was followed to assess the total antioxidant capacity of EAF and HSNPs. Briefly, 0.3 ml of EAF/HSNPs in methanol (1 mg/ml) and ascorbic acid (50-300 µg/ml) were mixed separately with 3 ml of study reagent (0.6 M H_2SO_4, 28 mM Na_3PO_4 and 4 mM $(NH_4)_6Mo_7O_{24}$). All the tubes were sealed and incubated in a boiling water bath at 95°C for 90 min. After cooling to room temperature, the absorbance of each sample was measured at 695 nm against the blank (3 ml of reagent solution+0.3 ml methanol). The total antioxidant capacity was expressed as the number of equivalents of ascorbic acid.

DPPH Free Radical Scavenging Activity

The free radical scavenging capacity of EAF/HSNPs was assessed by the 1, 1-diphenyl-2-picryl-hydrazil (DPPH) method.[39] In brief, 5 ml of DPPH solution (100 µM/ml in methanol) was added to 1ml of sample

in different concentrations (25–200 µg/ml). The absorbance was than measured after 30 min at 517 nm. The free radical scavenging activity was calculated using the following equation:

$$DPPH\ scavenging\ effect = 1 - \frac{A_1}{A_0} \times 100 \quad \text{(Equation 1)}$$

Where, A_0 is the absorbance of the blank and A_1 is the absorbance of test solution. Further, percent inhibition was plotted and IC_{50} was calculated with respect to ascorbic acid (positive control).

Scavenging of hydrogen peroxide

Scavenging capacity of EAF/HSNPs was determined using the method by Jayaprakasha *et al.*[40] A 20 mM solution of hydrogen peroxide (H_2O_2) was prepared in phosphate buffered saline (PBS, pH 7.4). Then, 1 ml EAF/HSNPs in varying concentrations and standards in methanol were added to 2 ml of above H_2O_2 solution. At last, after 10 min incubation, the absorbance was recorded at 230 nm. All readings were recorded in triplicates and then the calculation for percentage inhibition was done.

Assay for reducing power

Assay for reducing power was carried out by potassium ferricyanide method.[41] Briefly, 1 ml of EAF/HSNPs (final concentration 25-200 µg/ml) were admixed with 2.5 ml PBS (0.2M, pH 6.6) and 2.5 ml $K_3Fe(CN)_6$ (10 g/L). The resulting mixture was then incubated for 20 minutes at 50 ℃. To this, 2.5 ml of trichloroacetic acid (100 g/L) was incorporated, then centrifuged for 10 min at 300 rpm. Finally, the supernatant solution (2.5 ml) was collected followed by mixing with DW (2.5 ml) and 0.5 ml of $FeCl_3$ (1 g/L) and absorbance was recorded at 700 nm. Ascorbic acid served as positive control and PBS as a blank solution.

Nitric oxide scavenging assay

Nitric oxide scavenging assay was done using sodium nitroprusside.[42] In brief, 2 ml (10 mM) sodium nitroprusside in 0.5 ml PBS (pH 7.4) was admixed with varying concentrations of EAF/HSNPs (0.5 ml) and the mixture was then incubated at 25°C for about two and a half hours. Aliquot of 0.5 ml was taken out from the above mixture and added to 1 ml of sulfanilic acid (SA) reagent (33% SA in 20% glacial acetic acid) and again incubated at 25°C for 5 min. Finally, 1 ml naphthyl ethylenediamine dihydrochloride (0.1% w/v) was added and left for 30 min at 25°C. At last, the absorbance was recorded at 546 nm. The nitric oxide radical scavenging activity was calculated and percentage inhibition and IC_{50} was calculated using rutin, as positive control.

Scavenging of hydroxyl radical by deoxyribose method

Hydroxyl radical scavenging capacity of EAF/HSNPs was determined by assessing degradation of Deoxyribose.[43] The final reaction mixture (1.2 ml) contained the aliquots (0.2 ml) of varying concentrations of the EAF/HSNPs, ferric chloride (0.1 mM, 0.2 ml), EDTA (0.1 mM, 0.2 ml), ascorbic acid (0.1 mM, 0.2 ml) and H_2O_2 (2 mM, 0.2 ml) in PBS (pH, 7.4, 20 mM). These mixtures were then incubated at 37°C for 30 min. Thereafter, 0.2 ml of ice-cold trichloro acetic acid (15%, w/v) and 0.2 ml thiobarbituric acid (1% w/v in 0.25 N HCl) were added to the reaction mixtures and kept in a boiling water bath. After 30 minutes, the reaction mixtures were taken off and the absorbance was measured at 532 nm when the reaction mixture was cool. All the absorbance was recorded in triplicates and the percentage inhibition was calculated using equation (1).

Antibacterial activity

MIC of HSNPs was determined using CLSI M07-A7 (Nutrient Broth dilution) method.[44] In each of the twenty test tubes (previously sterilised and dried), 5 ml of sterilised Nutrient Broth (NB) was added. In first 8 test tubes, 1 ml of different concentrations of synthesised HSNPs suspension ranging from 10 µg/ml to 80 µg/ml were added respectively and marked as Gram +ve. The same was repeated for another 8 test tubes, marked as Gram –ve. The remaining 4 tubes were kept as blank, drug control (only HSNPs suspension), G+ve control and G–ve control respectively. Furthermore, 1ml (10^8 CFU/ml, 0.5 McFarland's standard) of G+ve strain (*Streptococcus aureus*) was added in each G+ve tube and 1mL (10^8 CFU/ml, 0.5 McFarland's standard) G–ve strain (*Escherichia coli*) was added in each G-ve tube except blank and drug control. Finally, the equal volume (7 ml) in each tube was maintained by adding distilled water and then, incubated at 37°C for 24 hours. After incubation, the MIC was measured by observing the turbidity.[45,46] Tests for EAF and Gentamicin (standard drug) were performed in similar fashion as HSNPs.

The antimicrobial activity of HSNPs was determined against *S. aureus* ATCC 25923 (Gram positive) and *E. coli* ATCC 25922 (Gram negative) bacterial strains by agar disk diffusion method as described by the clinical laboratory standards institute.[47] Briefly, colonies from an overnight culture of tested bacteria grown on nutrient agar were suspended in 3 ml saline and turbidity was adjusted to 0.5 McFarland ($1–2 \times 10^8$ CFU ml^{-1}) and uniformly spread with the help of sterile swab stick on MHA plates. Then, 40 µl of HSNPs, EAF, blank and Positive Control Gentamicin Disk (10 µg) was added on each culture-loaded MHA plate. All the sample loaded plates were incubated at 37°C for 18 h. After incubation, the zone of inhibition was measured and recorded in millimeters.

In vitro anti-inflammatory activity

With slight modifications, the *in vitro* anti-inflammatory potential of EAF and HSNPs was determined as per previous reports by assessing the inhibition of protein (albumin) denaturation and antiproteinase activity.[48,49] EAF and HSNPs were serially diluted in deionised water (DW) from 200 to 1200 µg/ml for protein denaturation and 100 to 1000 µg/ml respectively. Aspirin (100 µg/ ml, Sigma-Aldrich, Singapore), a standard anti-inflammatory drug, was used as a positive control, whereas DW was used as a negative control.

Inhibition of albumin denaturation

The reaction mixture, containing 1ml of one percent solution of bovine albumin fraction in water was added into 1 ml of EAF/HSNPs solution. This reaction mixture was incubated for 20 min at 37°C followed by heating to 51°C for 30 min after adjusting the pH 6.3. Thereafter, the reaction mixture was allowed to cool to room temperature, then absorbance was measured at 660 nm (Agilent UV-Vis Spectrophotometer). The following equation was used for calculating percentage inhibition of protein denaturation, and the concentration required for a 50% inhibition was expressed as IC_{50} values:

$$Percentage\ inhibition\ (\%) = \frac{A_{Control} - A_{Sample}}{A_{Control}} \times 100$$

Where, $A_{control}$ is the absorbance of DW and A_{sample} is the absorbance of the EAF/HSNPs.

Antiproteinase activity

The reaction mixture was prepared by adding 0.06 mg trypsin followed by 1mL of EAF/HSNPs into 1 mL of 20 mM Tris HCl buffer (pH 7.4) and incubated at 37°C for 5 min. To this, 1 mL of 0.8% (w/v) casein was then added and further incubated for 20 min. At last, the reaction was terminated by adding 2 mL perchloric acid (70%) and the mixture was centrifuged at 4°C, 6,000 rpm, for 10 min. The supernatant was collected, and absorbance was measured at 210 nm (Agilent UV-Vis

Spectrophotometer). The percent proteinase inhibition was calculated using the equation given below, and the results were expressed as IC_{50} values:

$$Percentage\ inhibition\ (\%) = \frac{A_{Control} - A_{Sample}}{A_{Control}} \times 100$$

Statistical analysis

The experimental results are represented as mean ± SEM (n=6). The statistical analysis was carried by one-way ANOVA with Tukey's post-hoc test, using GraphPad Prism software (version: 5.03, San Diego, USA). The data considered to be statistically significant $p < 0.05$.

RESULTS

Standardization of EBL fractions and quantification of campesterol in EAF

The HPTLC fingerprint of EBL and its fractions (AF, EAF, HF, BuOHF, DCMF) for qualitative analysis and quantitative analysis were represented in Fig. 2A & Fig. 2B, respectively. The fingerprinting analysis revealed the presence of various compounds especially terpenoids and steroidal constituents (Figure 2A). EAF showed a greater number of spots with high area of peaks indicating a greater number of constituents being isolated as compared to other fractions. The amount of Campesterol in the bands were estimated from the linear regression equation ($y= 8.89 \times 10^{-9}x$) obtained from amount per spot v/s respective area. Campesterol was quantified in EBL as well as EAF and was found to be 4.396±0.2 mg/g and 18.850±0.02 mg/g respectively (Figure 2B).

Synthesis and confirmation of HSNPs

In the current work, an attempt has been made to perform green synthesis of HSNPs involving EAF obtained from EBL. The colour change from buff yellow to reddish brown within 24 hours was indicative of HSNPs synthesis (Figure 3). Green synthesized HSNPs were then examined and primarily confirmed using UV-Visible spectrophotometry. Upon analysis, the green synthesized HSNPs showed absorption maximum (λ_{max}) at 441 nm while $AgNO_3$ solution had no such peak in visible range, as shown in Figure 4.

Characterization of HSNPs

ATR-FTIR analysis

The active functional groups present in plant extracts which were responsible for the reduction of Ag^+ to HSNPs were analysed by ATR-FTIR. The FTIR spectra (Figure 5) of both plant extracts and synthesized HSNPs showed the peaks at 3324 cm^{-1}, 2116 cm^{-1} and 1641 cm^{-1}. The peaks at 3324 cm^{-1} were responsible for the vibrational stretching of O-H bond of alcoholic or other phenolic groups like flavonoids present in both extracts and synthesized particles. The peaks at 2116 cm^{-1} and 1641 cm^{-1} were responsible for the vibrational stretching of C-H bond and CO bond of phytochemicals which were also present on HSNPs. The characteristic peak was at 1101 cm^{-1} which was present only in plant extracts, but the peak was vanished in synthesized particles. The peak at 1101 cm^{-1} was responsible for the vibration stretching of C-O bond of phytoconstituents which might be responsible for the reduction of Ag^+ to HSNPs. Hence form the FTIR spectra it might be speculated that phytoconstituents were responsible for the reduction of Ag^+ to HSNPs. Furthermore, the retention of the functional groups of phytoconstituents in the HSNPs represent the coating of phytoconstituents on the synthesized HSNPs.

Particle size analysis

The average hydrodynamic particle size of HSNPs was measured using dynamic light scattering (DLS) instrument after suitable dilution. The average size of particles was found to be 59.21 nm which due to bio reduction of Ag^+ ion to Ag^0. The polydisperse index (PDI) of HSNPs distribution was found to be 0.232. A PDI value of 0.1 to 0.25 represents a narrow size distribution, whereas a PDI greater than 0.5 represents a broad distribution.[50] The lower PDI value represents the narrow size distribution and monodisperse nature of the synthesized HSNPs.

TEM

TEM photomicrograph (Figure 6A) showed the size and shape of green synthesised HSNPs. The images revealed that the HSNPs were mostly spherical in shape and the particles were monodisperive. The average particle size of HSNPs was found to be 25 nm from the particle size distribution histogram using TEM images. The crystallinity of HSNPs was revealed by the bright dotted ring of the SAED image (Figure 6B).

SEM

The SEM results (Figure 7A) revealed the spherical shaped particles with most of the particles within the range of 20-80 nm. However, the presence of some large sized particles was due to their aggregation during drying process.

The average particles size was found in the range of 20-30 nm from the histogram (Figure 7B) showing the distribution of different size of particles which were measured by ImageJ software. The result of SEM was in accordance with the TEM and DLS results. The EDS results revealed the presence of Ag, N and C with their atomic percentage of 67.89%, 22.05% and 10.06%, respectively. The presence of elements other than Ag in the EDS analysis revealed that the phytoconstituents were responsible for the synthesis and capping of HSNPs (Figure 7C). The percentage of oxygen was not found in the EDS spectrum which revealed that synthesized HSNPs prevent oxidation.

X-ray diffraction (XRD) analysis

The XRD diffraction pattern of the HSNPs is shown in Figure 8. Highly intense sharp peaks of the HSNPs represents its crystallinity nature. High intensity diffraction peaks of HSNPs at 2Θ angles 38.50°, 44.94°, 64.50° and 76.60° were assigned to (1 1 1), (2 0 0), (2 2 0) and (3 1 1) reflections

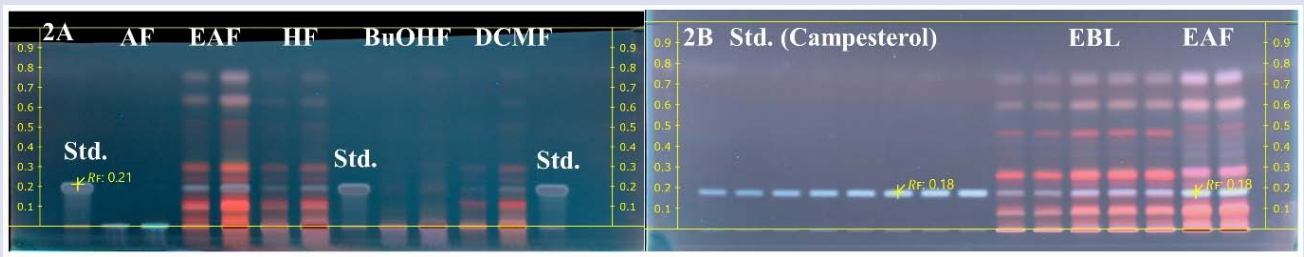

Figure 2: A) HPTLC fingerprinting analysis of all five fractions of EBL B) Quantification of campesterol in EBL and EAF.

Figure 3: Synthesis of HSNPs A) Starting of reduction process, B) After 24 hours of reduction.

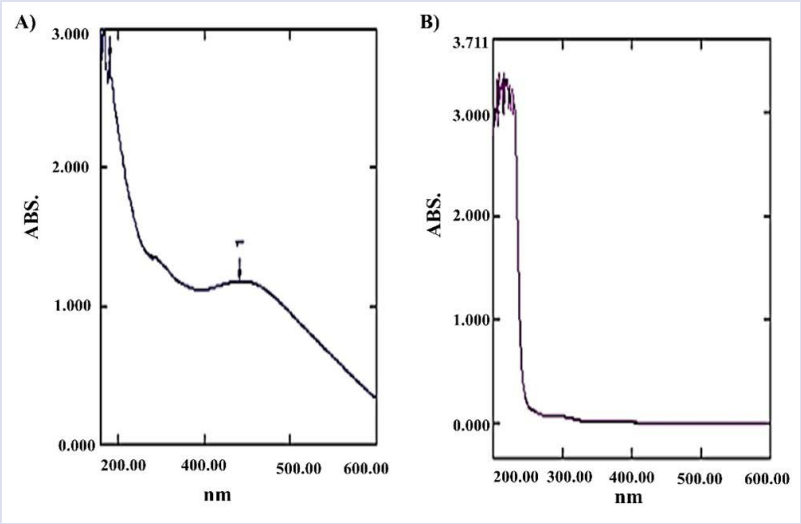

Figure 4: UV–vis spectrum of A) Synthesized HSNPs B) $AgNO_3$ solution.

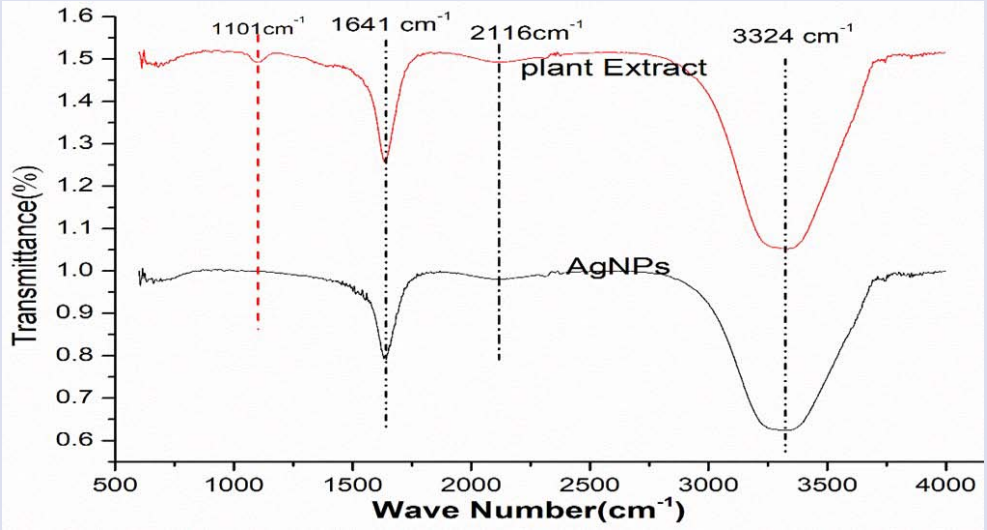

Figure 5: ATR-FTIR spectra of plant extracts (Red) and HSNPs (black).

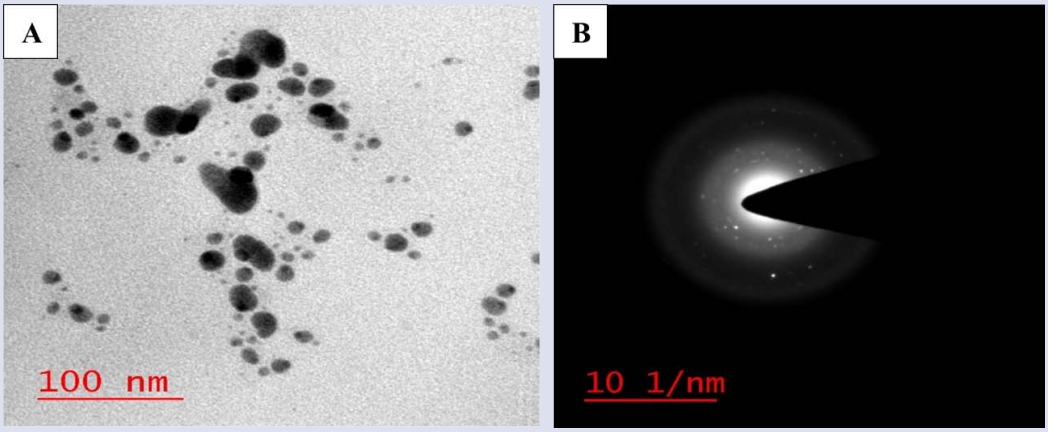

Figure 6: TEM images of (A) HSNPs and (B) SAED pattern.

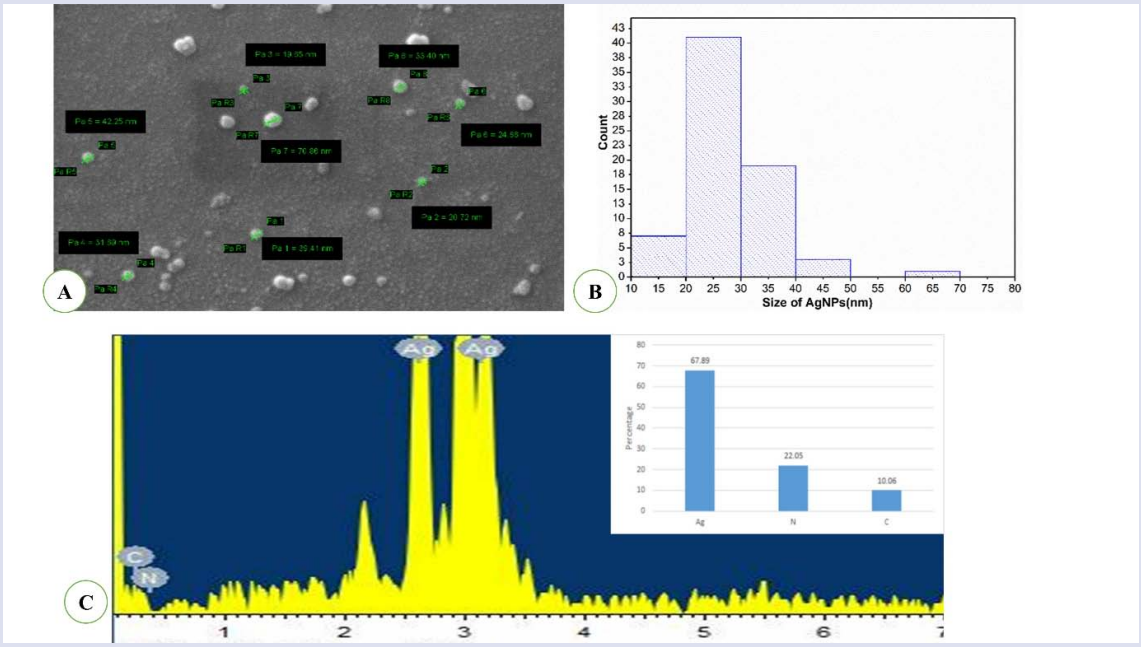

Figure 7: SEM image of HSNPs: A) Shape and Size, B) Distribution of different size HSNPs and C) EDAX analysis.

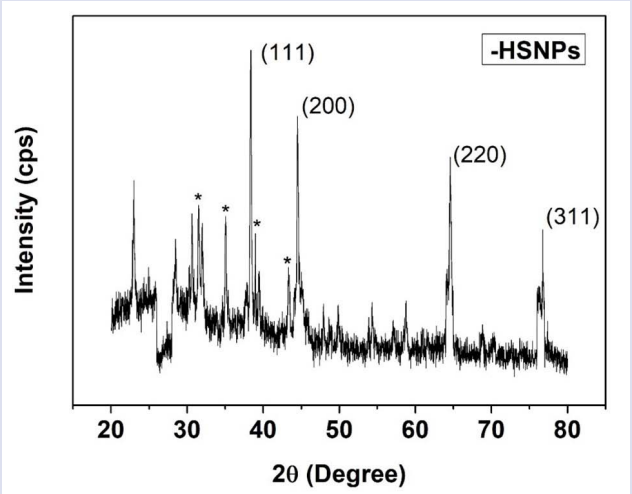

Figure 8: X-ray diffraction (XRD) pattern of HSNPs exhibiting orientation of nanoparticles towards plate 111 (parenthesis).

of the face-cantered cubic (FCC) structure as per the Joint Committee on Powder Diffraction Standards (JCPDS file No. 04-0783) [51,52]. The orientation of the HSNPs were found towards plate 111 confirming its crystalline nature. The peaks assigned as asterisks in figure are the one obtained due to crystallization phytoconstituents present on HSNPs surface. Thus, encapsulation of HSNPs by phytoconstituents present in EAF was confirmed supplementing the EDS results.

Quantitative estimation of various classes of phytoconstituents

The results of quantitative estimation of HSNPs and all five fractions of EBL is given in Table 1. The test results confirmed total phenolic content as 207.859±6.28 mg/g gallic acid equivalent in HSNPs. Total flavonoids and flavonol content were found to be 146.931±8.76 mg/g and 24.482±8.76 mg/g equivalent to rutin respectively in HSNPs.

Estimation of entrapment efficiency and drug loading capacity

The entrapment efficiency HSNPs was found to be 86.85% while the loading capacity was found to be 3.474%.

In vitro release profile of HSNPs

Release of campesterol from HSNPs has been shown in Figure 9. The release pattern of campesterol was found to be rapid, as a liminal burst release was observed irrefutably in the first 4 hours in both the media. This release pattern could be expedient in ameliorating hemorrhoids by attaining the desired threshold of action rapidly. Almost 50% of release of campesterol in the first 4 hours was noted, with comparatively slower release rate afterwards. An explication to this can be a rapid release of phytoconstituents capped on the outer surface followed by the release of phytoconstituents encapsulated in the core of HSNPs.[5,11]

PHARMACOLOGICAL SCREENING

In vitro antioxidant activity

The results of the total antioxidant capacity, reducing power and scavenging activity of DPPH, hydrogen peroxide and hydroxyl radical for EAF and HSNPs have been represented respectively in Table 2. The total antioxidant capacity was determined by linear regression equation and was expressed as number of equivalents of ascorbic acid. Total Antioxidant capacity of EAF and HSNPs was found to be 92.46 ± 1.91

Table 1: Quantitative estimation of various classes of phytoconstituents.

Sample	Total phenolic content (mg/g GAE)*	Total flavonoid content (mg/g RE)*	Total flavonol content (mg/g RE)*
Hexane fraction (HF)	224.566± 6.19	186.371± 10.39	34.877± 5.80
Ethyl Acetate fraction (EAF)	377.601± 4.00	248.564±6.77	51.116± 5.76
Dichloromethane fraction (DCMF)	226.401± 7.57	215.625±3.34	38.495± 2.90
Butanol fraction (BuOH)	125.202± 5.93	65.499± 9.02	17.933± 1.27
HSNPs	207.859±6.28	146.931±8.76	24.482±8.76

*The results are average of three determinations ± SEM

Table 2: *In vitro* antioxidant activities of EBL.

Drug	IC_{50} ±SEM*(µg/ml)			
	DPPH radical	Nitric Oxide	H_2O_2 radical	Deoxyribose
Standard	Ascorbic acid	Rutin	Rutin	BHA
	46.58 ± 1.95	31.60 ± 1.84	14.21 ± 0.86	31.63 ± 1.91
Sample				
EA Fraction	57.92 ± 3.40	49.49 ± 3.64	27.45 ± 1.31	41.46 ± 1.84
HSNPs	75.36 ± 1.60	53.85 ± 3.09	33.57 ± 1.93	57.89 ± 2.27

*The results are average of three determinations ± SEM

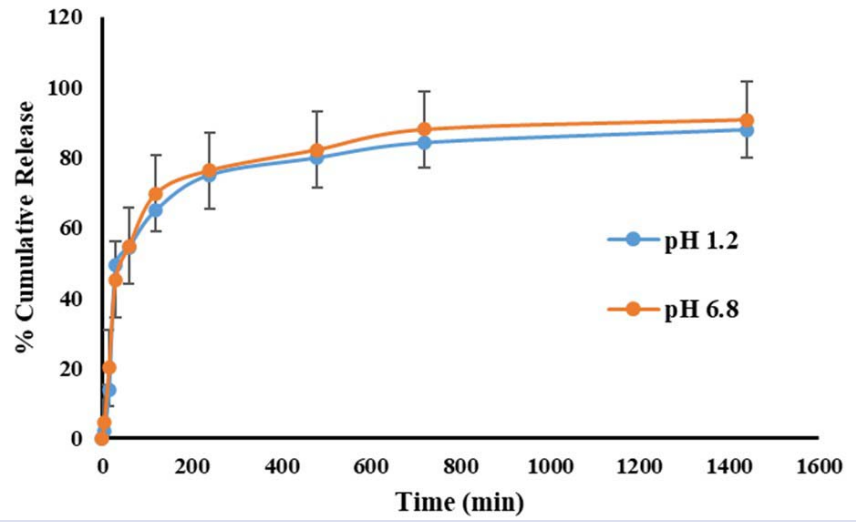

Figure 9: *In vitro* drug release profile of campesterol from HSNPs.

µg/ml and 82.78 ± 5.84 µg/ml respectively. Assay of reducing power is a concentration dependent reaction i.e.; higher concentration indicates higher reducing power. The results demonstrated a potent reducing potential of EAF (4.08 ±0.44 µg/ml) and HSNPs (3.43 ±0.56 µg/ml). The capability to reduce DPPH by donating an electron or hydrogen to DPPH is indicative of free radical scavenging activity of the extract. EAF and HSNPs showed an IC_{50} value of 61.00 ±1.60 µg/ml and 75.53 ±3.40 µg/ml as compared to ascorbic acid (IC_{50}: 46.58±1.94 µg/ml). Griess reagent was used to determine the nitric oxide scavenging activity, which illustrated a good scavenging activity of EAF (IC_{50}: 48.52 ±3.64 µg/ml) but moderate scavenging activity of HSNPs (IC_{50}: 53.39 ±3.09µg/ml) in comparison to rutin (IC_{50}: 31.92 ±1.84 µg/ml). A considerably moderate scavenging potential of hydrogen peroxide by HSNPs was observed with an IC_{50} value of 32.68 ±1.93 µg/mL compared to standard rutin ($IC_{50:}$ 15.29 ±0.86 µg/ml) while EAF showed good activity ($IC_{50:}$ 27.23 ±1.31 µg/ml). Fenton reaction was used to assess the potential of EAF and HSNPs in inhibiting the hydroxyl radical production through iron (II)–dependent deoxyribose damage assay. The results showed significant scavenging activity with an IC_{50} value of 42.37 ±1.84 µg/ml and 57.80 ±2.27 µg/ml compared to positive control BHA (IC_{50} 31.73 ± 1.91 µg/ml).

Antibacterial activity

The antimicrobial efficacy of HSNPs and EAF along with positive (gentamicin) and negative control (distilled water) were tested against respective Gram-positive (*S. aureus*) and Gram-negative (*E. coli*) pathogens using the agar well diffusion method and the results were presented in Figure 10. The zone of inhibitions on all pathogens was carefully measured after incubation of 24 h at 37°C. The result revealed that the HSNPs exhibited higher antibacterial activity in terms of zone of inhibition against *E. coli* and *S. aureus* pathogens when compared to the EAF. The maximum zone of inhibition against *E. coli* (18.3 ± 2.08 mm for 50 µg/ml) and *S. aureus* (25.0 ± 1.19 for 50 µg/ml) was observed in HSNPs treated wells. The EAF and antibiotic also displayed the antimicrobial activity of 15.0 ± 1.4 mm and 30.4 ± 1.39 mm against *E. coli* whereas 20.7 ± 1.21 mm and 33.1 ± 1.90 mm against *S. aureus*, respectively. The minimum inhibitory concentration (MIC) study using the micro broth dilution method revealed that the MIC of HSNPs against *E. coli* was found to be 30–80 µg/ml followed by EAF (50–80 µg/ml) and gentamicin (10–80 µg/ml) (Table 3). For *S. aureus* the MIC values were 20–80 µg/ml, 60–80 µg/ml and 10–80 µg/ml for HSNPs, EAF and gentamicin respectively (Table 3).

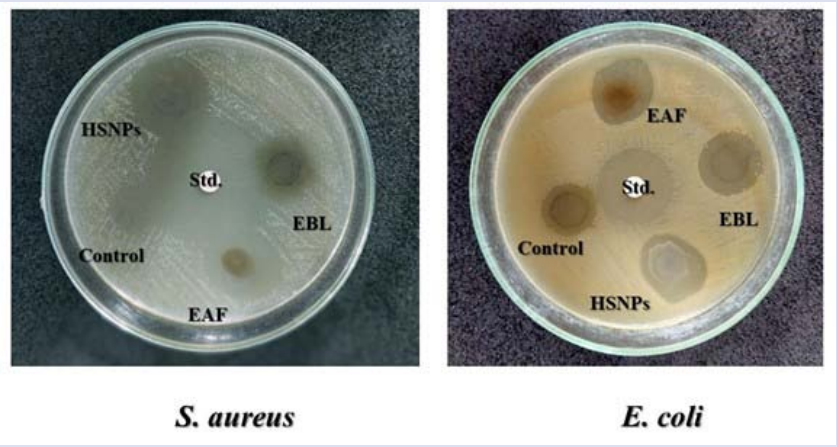

Figure 10: Antimicrobial activity of HSNPs.

Table 3: MIC value of HSNPs, EAF and Gentamicin against *E. coli* and *S. aureus*.

Drug		MIC* Concentration (µg/ml)							
		10	20	30	40	50	60	70	80
Gentamicin	*E. coli*	+	+	+	+	+	+	+	+
	S. aureus	+	+	+	+	+	+	+	+
EAF	*E. coli*	-	-	-	-	+	+	+	+
	S. aureus	-	-	-	-	-	+	+	+
HSNPs	*E. coli*	-	-	+	+	+	+	+	+
	S. aureus	-	+	+	+	+	+	+	+

*The results are average of three determinations ± SEM

Table 4: *In vitro* anti-inflammatory activity HSNPs, EAF and Aspirin.

Drug	IC_{50} ±SEM*(µg/ml)	
	Albumin denaturation	Anti-proteinase activity
Aspirin	50.56±4.010	46.61±2.80
EAF	93.97±5.646	96.41±5.95
HSNPs	61.57± 10.83	69.69± 5.00

*The results are average of three determinations ± SEM

In vitro anti-inflammatory activity

Inhibition of albumin denaturation

Loss of structure and function of a protein because of damage caused by physical, chemical, or biological means is called protein denaturation. Hence, tissue protein denaturation serves as indicator of inflammation. In current study, the *in vitro* anti-inflammatory potential of HSNPs and EAF was assessed through inhibition protein denaturation. As set forth in Table 4, HSNPs (IC_{50} 63.29 µg/ml) demonstrated the highest potential in preventing the albumin denaturation, followed by EAF with IC_{50} value of 93.65 µg/ml. The results are comparable with that of the standard drug aspirin.

Antiproteinase activity

Inflammatory reactions involve various agents such as proteinases. For example, leukocyte proteinases have significant role in tissue damage caused in inflammatory reactions. Hence, inhibition of these proteinases can help in protection of tissue damage. As given in Table 4, HSNPs (IC_{50} 69.56 µg/ml) corroborated the highest efficacy in preventing the proteinases, followed by EAF with IC_{50} value of 94.99 µg/ml. The results are comparable with that of the standard drug aspirin.

DISCUSSION

Nanoscale based formulations has attracted the scientists worldwide because of its wide range of applicability, lesser toxicity and more palatability.[53] Biogenic and bio-fabricated nanoparticles involve one step-one pot process for their synthesis. This method of nanoparticles synthesis is cheaper, less hazardous, and less tedious.

As per previous reports, *Blumea lacera* is claimed to possess antioxidant, antimicrobial, anti-inflammatory and anti-hemorrhoid activity.[14] There is lack of established scientific reports for the synthesis of bio-fabricated silver nanoparticles involving *Blumea lacera* and its medical applicability. Hence, the investigators report the synthesis, characterization, and evaluation of biological potency of silver nanoparticles (HSNPs) from EBL in this study.

Polyphenol enriched plants are generally preferred for biogenic nanoparticles synthesis as high number of flavonoids and sterols could yield greater amount of HSNPs.[54-56] Therefore, all the five fractions of EBL were quantified for campesterol through HPTLC and for total phenolics, flavonoids and flavanols through chemical methods. The results suggested that ethyl acetate fraction possessed highest content of total phenolics, flavonoids as well as flavanols and campesterol. However, HSNPs were noted to have comparatively less amount of the aforesaid groups that might be due to consumption during formation of HSNPs. Reduction of Ag^{+} ions to Ag^{0} upon adding EAF into $AgNO_3$ solution was noted after observing a change in colour from buff yellow to reddish brown (Figure 3).

Formation of HSNPs was confirmed by observing the characteristic peak at 441 nm in the spectra using UV-visible absorption spectroscopy: a prominent analytical tool for measuring SPR and for investigation of the optical properties of HSNPs. The peak at 441 nm shown by HSNPs, in the current study, was within the range (400-480 nm) of the characteristic SPR exhibited by silver nanoparticles.[57] The results of XRD revealed the pattern of HSNPs suggestive of crystalline nature of the particles. The intense diffraction peaks at (111), (200), (220) and (311), for HSNPs were in accordance with the Joint Committee on Powder Diffraction Standards (JCPDS) file no. 04-0783 for silver. For determining different functional groups FT-IR spectroscopy is applied. In the current study, FT-IR analysis was done to determine the plausible phytoconstituents from EAF which are primarily involved in reduction of $AgNO_3$ and formation of HSNPs along with capping on its surface. The results of FTIR showed the presence of hydroxyl and carbonyl functional groups, indicating the presence of phytosterols and flavonoids in the stabilized HSNPs.[58] As per reports, the carbonyl and hydroxyl groups present in campesterol and other sterols might be responsible for nanoparticle formation involving the mechanism of nucleation, complexation and dimerization.[59,60] SEM and TEM characterization results demonstrated the smooth, uniform, monodispersed, spherical shape of HSNPs. In the SAED pattern, polycrystalline nature of the HSNPs were observed which were compliant to the XRD results and earlier studies.[61,62] The average particle size of HSNPs was found to be 25nm from the particle size distribution histogram. Although, minimal agglomeration has been observed indicating the presence of phytoconstituents on HSNPs surface.

Drug loading capacity is defined as the ratio of the practically determined percentage of drug content as compared to theoretical mass of drug used in the formulation of the nanoparticles.[63] The drug loading capacity is dependent on the polymer-drug combination and the method applied. Hydrophobic polymers tend to encapsulate larger amounts of hydrophobic drug and vice-versa.[63] Several formulation factors, such as type of stabilizing agent and polymer-drug mass ratio will influence the extent of drug loading.[64]

During drug development process it becomes necessary establish the behaviour and assure the quality of the drug as well as *in vitro in vivo* correlation (IVIVC), hence *in vitro* drug release kinetics becomes an important tool for assessing the aforementioned parameters.[65] In current investigation, the release pattern of campesterol from HSNPs was observed which revealed that the release of campesterol was faster at first enabling it to acquire rapid onset of action but was slower at later stage extending its mean residence time (MRD). This release behaviour of campesterol is supporting the claim of capping the HSNPs.

Overproduction of reactive oxygen species (ROS) can alter the anatomy and physiology of various vital organs by damaging the DNA, proteins, tissues and neurotransmitter signalling pathways.[66] The role ROS in aetiology of various diseases have been established by many researchers.[67,68] Drugs with natural origin possess high antioxidant capacity, therefore, the biogenic HSNPs along with EAF have been evaluated for their antioxidant potential in this study. The results showed that the HSNPs had less antioxidant effect than that of EAF, but the difference was non-significant. One of the major reasons behind this may be the loss of polyphenols and sterols during the reduction of $AgNO_3$ for the formation HSNPs.

Search for new antimicrobials to combat the resistance developed by microorganisms has been one of the major thrust areas of drug discovery. Nanoparticles being smaller in size with high surface area are a better alternate for conventional antimicrobial agents. Moreover, the biogenic nanoparticles capped with phytoconstituents can act on microorganisms through several simultaneous mechanisms preventing the development of resistance by the microbes.[69,70] The results of antibacterial assay showed that the HSNPs have significant antimicrobial activity against both types (G- & G+) of pathogens when compared to EAF, this may be attributed to spherical shape and smaller size of HSNPs. The smaller size of HSNPs enables it to react with sulphur and phosphorus groups of amino acids on the cell membrane which in turn alters the surveillance of bacteria and to penetrate the cell wall of bacteria.[71,72] Furthermore, ionic silver from HSNPs gets attached to negatively charged particles on bacterial cell wall which leads to change in the cell wall composition ultimately affecting cell permeability.[72]

Inflammatory response to any kind external stimuli that causes alteration to normal anatomy and physiology of human tissue is the natural defence mechanism of human physiological system. This inflammatory response is very complex that involves several factors which may be associated with several diseases. However, use of steroidal

and nonsteroidal anti-inflammatory drugs (NSAIDs) for the treatment of inflammation is common but use of these drugs causes serious side effects.[49,73] Hence, in search of a better natural anti-inflammatory drug with lesser adverse events, the potential of HSNPs as anti-inflammatory drugs have been evaluated. As evident from the results, HSNPs possess high efficacy as anti-inflammatory agent than EAF and may be good alternative to combat the complications caused during inflammation. These anti-inflammatory property of HSNPs may be due to the retainment of phytosterols on the surface of HSNPs as these constituents have been studied rigorously as anti-inflammatory agents acting through several mechanisms such as phagocytosis, suppression of cytokines (TNF-α) production and also inflammatory mediators like COX-2 and Inos.[74,75]

CONCLUSION

The current study focused on the green synthesis of HSNPs utilising the EAF fraction prepared from ethanolic extract of *Blumea lacera*. Upon characterization, the HSNPs showed spherical shape with average particle size of 20-30 nm. Phytochemical analysis of the fraction revealed the presence of phenolic compounds, sterols, and flavonoids responsible for reduction and capping of HSNPs. Later, the release pattern of campesterol from HSNPs confirmed the above observation. From the results of antioxidant, anti-bacterial and *in-vitro* anti-inflammatory activity, it is evident that HSNPs can be good alternative to the currently used medicines for treating bacterial infections and inflammation. Therefore, it can be concluded that biological synthesis of HSNPs using EAF from EBL is efficient and economical process and HSNPs synthesized through this process can be potential agents in amelioration of various inflammation related pathological conditions. Although, more rigorous *in-vivo* studies need to be conducted in future to get deep insight of the actual mechanism taking place behind these pharmacological activities.

ACKNOWLEDGMENT

The authors highly acknowledge Department of Pharmaceutical Engineering and Technology, Indian Institute of Technology (Banaras Hindu University), Varanasi for infrastructural facility and Central Instrument Facility, IIT (BHU), Varanasi, for instrumental services.

Authors Contributions: Conceptualization, methodology, data collection, investigation, analysis, validation, interpretation, and preparation of Original Draft: Tarkeshwar Dubey; Validation, Formal analysis, experimentation, editing, and scientific modification of the manuscript: Kancharla Bhanukiran and Kuna Das; Conceptualization, Supervision, interpretation of data & concluding the results, technical support, and manuscript review: Siva Hemalatha.

Funding: The financial support in the form of scholarship was provided to Tarkeshwar Dubey for this work by the Ministry of Human Resource Development (MHRD), Government of India.

Data Availability: All data recorded and generated during this research are included in this article.

Code Availability: All the data were produced using MS office package, a 21-day free trial version of Origin Pro 2021 (Microcal Software, Inc., Northampton, Northampton, MA, USA), and ImageJ software (National Institutes of Health, Bethesda, MD).

DECLARATIONS

Conflict Of Interest: The authors report no conflicts of interest and are solely responsible for this manuscript.

Ethical Approval: Not applicable.

Consent to Participate Not applicable.

Consent for Publication Not applicable.

REFERENCES

1. Srivastava S, Bhargava A. Nanobiotechnology: Present Status and Future Prospects. Green Nanoparticles: The Future of Nanobiotechnology: Springer. 2022;345-52.
2. Larue C, Castillo-Michel H, Sobanska S, Cécillon L, Bureau S, Barthès V, *et al*. Foliar exposure of the crop Lactuca sativa to silver nanoparticles: evidence for internalization and changes in Ag speciation. J Hazardous Materials. 2014;264:98-106.
3. Dikshit PK, Kumar J, Das AK, Sadhu S, Sharma S, Singh S, *et al*. Green synthesis of metallic nanoparticles: applications and limitations. Catalysts. 2021;11(8):902.
4. Ahmed S, Ahmad M, Swami BL, Ikram S. A review on plants extract mediated synthesis of silver nanoparticles for antimicrobial applications: a green expertise. J Adv Res. 2016;7(1):17-28.
5. Ovais M, Khalil AT, Raza A, Khan MA, Ahmad I, Islam NU, *et al*. Green synthesis of silver nanoparticles via plant extracts: beginning a new era in cancer theranostics. Nanomed. 2016;12(23):3157-77.
6. Yu Y, Zhang Q, Yao Q, Zhan Y, Lu M, Yang L, *et al*. Learning from nature: introducing an epiphyte–host relationship in the synthesis of alloy nanoparticles by co-reduction methods. ChemComm. 2014;50(68):9765-8.
7. Moradi F, Sedaghat S, Moradi O, Arab Salmanabadi S. Review on green nano-biosynthesis of silver nanoparticles and their biological activities: with an emphasis on medicinal plants. Inorg Nano-Met Chem. 2021;51(1):133-42.
8. Zaheer Z. Bio-conjugated silver nanoparticles: from Ocimum sanctum and role of cetyltrimethyl ammonium bromide. Colloids Surf B Biointerfaces. 2013;108(1):90-4.
9. Jacob SJP, Finub J, Narayanan A. Synthesis of silver nanoparticles using Piper longum leaf extracts and its cytotoxic activity against Hep-2 cell line. Colloids Surf B Biointerfaces. 2012;91(1):212-4.
10. Dipankar C, Murugan S. The green synthesis, characterization and evaluation of the biological activities of silver nanoparticles synthesized from Iresine herbstii leaf aqueous extracts. Colloids Surf B Biointerfaces. 2012;98(1):112-9.
11. Makarov V, Love A, Sinitsyna O, Makarova S, Yaminsky I, Taliansky M, *et al*. "Green" nanotechnologies: synthesis of metal nanoparticles using plants. Acta Naturae. 2014;6(20):35-44.
12. Vattem DA, Ghaedian R, Shetty K. Enhancing health benefits of berries through phenolic antioxidant enrichment: focus on cranberry. Asia Pac J Clin Nutr. 2005;14(2):120.
13. Dubey T, Bhanukiran K, Hemalatha S. Quality Control Standardization of Blumea lacera (Burm. f.) DC. Leaves. Indian J Nat Prod. 2019;33(1):53-9.
14. Tarkeshwar Dubey SKJ, Siva Hemalatha. Blumea lacera (Asteraceae), a Potential Herb of Medicinal Value in Modern Aspects. In: Singh Bikarma SYP, editor. Ethnobotany to Ethnopharmacology: Exploiting Plants for Novel Drug Molecules. New Delhi, India: New India Publishing Agency; 2021;397-410.
15. Beg A. Antifungal assay of some angiospermic plant extract against Fusarium lycopersicum. Indian J Applied & Pure Bio. 2011;26(1):71-4.
16. Mahajan R. Ethnobotanical Significance and Antimicrobial Activity of Blumea lacera (Roxb.) DC. Int J Pharm Biol Arch. 2010;1(3):314-6.
17. Natarajan B, Paulsen BS. An ethnopharmacological study from Thane district, Maharashtra, India: Traditional knowledge compared with modern biological science. Pharm Biol. 2000;38(2):139-51.
18. Manandhar NP. An inventory of some herbal drugs of Myagdi district, Nepal. Econ Bot. 1995;49(4):371-9.

19. Pandey AK, Tripathi N. Aromatic Plants of Gorakhpur Division: Their Antimycotic Properties and Medicinal Value. Extraction. 2011;7(2):26.
20. Kumar B, Vijayakumar M, Govindarajan R, Pushpangadan P. Ethnopharmacological approaches to wound healing—exploring medicinal plants of India. J Ethnopharmacol. 2007;114(2):103-13.
21. Mollik MAH, Hossan MS, Paul AK, Taufiq-Ur-Rahman M, Jahan R, Rahmatullah M. A comparative analysis of medicinal plants used by folk medicinal healers in three districts of Bangladesh and inquiry as to mode of selection of medicinal plants. Ethnobot Res Appl. 2010;8(1):195-218.
22. Sen SK, Behera LM. Ethnomedicinal plants used by the tribals of Bargarh district to cure diarrhoea and dysentery. Indian J Tradit Knowl. 2008;7(3):425-8.
23. Prasad R, Lawania RD, Gupta R. Role of herbs in the management of asthma. Pharmacogn Rev. 2009;3(6):247.
24. Rahman A. Medico-botanical study of the plants found in the Rajshahi district of Bangladesh. Prud J Med Plants Res. 2013;1(1):1-8.
25. Korpenwar A. Ethnomedicinal plants used by bhilala tribals in buldhana district (MS). DAVIJS. 2012;1(1):60-5.
26. Singh AP. Ethnobotanical Studies of Chandigarh Region. Ethnobot leafl. 2005;2005(1):33.
27. Khare CP. Indian herbal remedies: rational Western therapy, ayurvedic, and other traditional usage, Botany: Springer science & business media. 2004.
28. Mukherjee SK, editor Medicinal plants of Asteraceae in India and their uses. Proceeding of National Seminar; Gupta, SK, Mitra, BR, Eds; 2006.
29. Tiwari Pawan, Saluja Gurdeep, Pandey Ajay Shankar, Naveen S. Isolation and biological evaluation of some novel phytoconstituents from blumea lacera (burn f.) dc. Int J Pharm Pharm Sci. 2012;4(4):148-50.
30. Ragasa CY, Wong J, Rideout JA. Monoterpene glycoside and flavonoids from Blumea lacera. J Nat Med. 2007;61(4):474-5.
31. Capasso F, Cerri R, Morrica P, Senatore F. Chemical composition and anti-inflammatory activity of an alcoholic extract of Teucrium polium L. Boll Soc Ital Biol Sper. 1983;59(11):1639-43.
32. Utami W, Aziz H, Fitriani I, Zikri A, Mayasri A, Nasrudin D. In silico anti-inflammatory activity evaluation of some bioactive compound from ficus religiosa through molecular docking approach. Journal of Physics: Conference Series; 2020: IOP Publishing.
33. Parvu A, Parvu M, Vlase L, Miclea P, Mot A, Silaghi-Dumitrescu R. Anti-inflammatory effects of Allium schoenoprasum L. leaves. J Physiol Pharmacol. 2014;65(2):309-15.
34. Hassan EM, Matloub AA, Aboutabl ME, Ibrahim NA, Mohamed SM. Assessment of anti-inflammatory, antinociceptive, immunomodulatory, and antioxidant activities of Cajanus cajan L. seeds cultivated in Egypt and its phytochemical composition. Pharm Biol. 2016;54(8):1380-91.
35. Chavan RR, Bhinge SD, Bhutkar MA, Randive DS, Wadkar GH, Todkar SS. In vivo and in vitro hair growth-promoting effect of silver and iron nanoparticles synthesized via Blumea eriantha DC plant extract. J Cosmet Dermatol. 2021;20(4):1283-97.
36. Hagerman A. Quantification of tannins in tree foliage: a laboratory manual for the FAO/IAEA co-ordinated research project on" The use of nuclear and related techniques to develop simple tannin assays for predicting and improving the safety and efficiency of feeding ruminants on tanninferous tree foliage. http://www iaea org/programmes/nafa/d3/crp/pubd31022manual-tannin pdf. 2000.
37. Kumaran A, Karunakaran RJ. In vitro antioxidant activities of methanol extracts of five Phyllanthus species from India. LWT. 2007;40(2):344-52.
38. Prieto P, Pineda M, Aguilar M. Spectrophotometric quantitation of antioxidant capacity through the formation of a phosphomolybdenum complex: specific application to the determination of vitamin E. Anal Biochem. 1999;269(2):337-41.
39. Blois MS. Antioxidant determinations by the use of a stable free radical. Nature. 1958;181(4617):1199-200.
40. Jayaprakasha GK, Rao LJ, Sakariah KK. Antioxidant activities of flavidin in different in vitro model systems. Bioorg Med Chem. 2004;12(19):5141-6.
41. Yıldırım A, Mavi A, Kara AA. Determination of antioxidant and antimicrobial activities of Rumex crispus L. extracts. J Agric Food Chem. 2001;49(8):4083-9.
42. Rao M. Nitric oxide scavenging by curcuminoids. J Pharm Pharmacol. 1997;49(1):105-7.
43. Halliwell B, Gutteridge JM, Aruoma OI. The deoxyribose method: a simple "test-tube" assay for determination of rate constants for reactions of hydroxyl radicals. Anal Biochem. 1987;165(1):215-9.
44. Wikler MA. Methods for dilution antimicrobial susceptibility tests for bacteria that grow aerobically: approved standard. CLSI (NCCLS). 2006;26(1):M7-A.
45. Standards NCfCL, Barry AL. Methods for determining bactericidal activity of antimicrobial agents: approved guideline: National Committee for Clinical Laboratory Standards Wayne, PA; 1999.
46. Balouiri M, Sadiki M, Ibnsouda SK. Methods for in vitro evaluating antimicrobial activity: A review. J Pharm Anal. 2016;6(2):71-9.
47. Clinical, Institute LS. Zone diameter interpretive standards, corresponding minimal inhibitory concentration (MIC) interpretive breakpoints, and quality control limits for antifungal disk diffusion susceptibility testing of yeasts; Informational supplement M44-S2. Clinical and Laboratory Standards Institute Wayne; 2009.
48. Oyedapo O, Famurewa AJ. Antiprotease and membrane stabilizing activities of extracts of Fagara zanthoxyloides, Olax subscorpioides and Tetrapleura tetraptera. IJP. 1995;33(1):65-9.
49. Truong D-H, Nguyen DH, Ta NTA, Bui AV, Do TH, Nguyen HC. Evaluation of the use of different solvents for phytochemical constituents, antioxidants, and in vitro anti-inflammatory activities of Severinia buxifolia. J Food Qual. 2019;2019.
50. Wu L, Zhang J, Watanabe W. Physical and chemical stability of drug nanoparticles. Advanced drug delivery reviews. 2011;63(6):456-69.
51. Peram MR, Jalalpure S, Kumbar V, Patil S, Joshi S, Bhat K, *et al.* Factorial design based curcumin ethosomal nanocarriers for the skin cancer delivery: in vitro evaluation. J Liposome Res. 2019;29(3):291-311.
52. Chavan RR, Bhinge SD, Bhutkar MA, Randive DS, Wadkar GH, Todkar SS, *et al.* Characterization, antioxidant, antimicrobial and cytotoxic activities of green synthesized silver and iron nanoparticles using alcoholic Blumea eriantha DC plant extract. Mater Today Commun. 2020;24(1):101320.
53. Saeedi M, Eslamifar M, Khezri K, Dizaj SM. Applications of nanotechnology in drug delivery to the central nervous system. Biomed Pharmacother. 2019;111:666-75.
54. Saratale RG, Shin H-S, Kumar G, Benelli G, Ghodake GS, Jiang YY, *et al.* Exploiting fruit byproducts for eco-friendly nanosynthesis: Citrus× clementina peel extract mediated fabrication of silver nanoparticles with high efficacy against microbial pathogens and rat glial tumor C6 cells. Environ Sci Pollut Res. 2018;25(11):10250-63.
55. Swilam N, Nematallah KA. Polyphenols profile of pomegranate leaves and their role in green synthesis of silver nanoparticles. Sci Rep. 2020;10(1):1-11.
56. Latif M, Abbas S, Kormin F, Mustafa M. Green synthesis of plant-mediated metal nanoparticles: The role of polyphenols. Asian J Pharmaceut Clin Res. 2019;12(7):75-84.

57. Nazeruddin G, Prasad N, Prasad S, Shaikh Y, Waghmare S, Adhyapak P. Coriandrum sativum seed extract assisted in situ green synthesis of silver nanoparticle and its anti-microbial activity. Ind Crops Prod. 2014;60:212-6.

58. Khan MA, Khan T, Nadhman A. Applications of plant terpenoids in the synthesis of colloidal silver nanoparticles. Adv Colloid Interface Sci. 2016;234:132-41.

59. Isa N, Lockman Z. Methylene blue dye removal on silver nanoparticles reduced by Kyllinga brevifolia. Environ Sci Pollut Res. 2019;26(11):11482-95.

60. Kumar KM, Mandal BK, Tammina SK. Green synthesis of nano platinum using naturally occurring polyphenols. RSC Adv. 2013;3(12):4033-9.

61. Velmurugan P, Shim J, Kim K, Oh B-T. Prunus× yedoensis tree gum mediated synthesis of platinum nanoparticles with antifungal activity against phytopathogens. Mater Lett. 2016;174:61-5.

62. Saratale RG, Benelli G, Kumar G, Kim DS, Saratale GD. Bio-fabrication of silver nanoparticles using the leaf extract of an ancient herbal medicine, dandelion (Taraxacum officinale), evaluation of their antioxidant, anticancer potential, and antimicrobial activity against phytopathogens. Environ Sci Pollut Res. 2018;25(11):10392-406.

63. Ndikau M, Noah NM, Andala DM, Masika E. Green synthesis and characterization of silver nanoparticles using Citrullus lanatus fruit rind extract. Int J Anal Chem. 2017;2017.

64. Lekshmi UD, Poovi G, Reddy PN. In-vitro observation of repaglinide engineered polymeric nanoparticles. Dig J Nanomater Bios. 2012;7(1):1-18.

65. D'Souza S. A review of in vitro drug release test methods for nano-sized dosage forms. Adv pharm. 2014;2014.

66. Dubey T, Sahu G, Kumari S, Yadav BS, Sahu AN. Role of herbal drugs on neurotransmitters for treating various CNS disorders: A review. Indian J Tradit Knowl. 2018;17:113-21.

67. Valko M, Leibfritz D, Moncol J, Cronin MT, Mazur M, Telser J. Free radicals and antioxidants in normal physiological functions and human disease. Int J Biochem Cell Biol. 2007;39(1):44-84.

68. Losada-Barreiro S, Bravo-Diaz C. Free radicals and polyphenols: The redox chemistry of neurodegenerative diseases. Eur J Med Chem. 2017;133:379-402.

69. Wang L, Hu C, Shao L. The antimicrobial activity of nanoparticles: present situation and prospects for the future. Int J Nanomed. 2017;12:1227-9.

70. Singh P, Garg A, Pandit S, Mokkapati V, Mijakovic I. Antimicrobial effects of biogenic nanoparticles. Nanomat. 2018;8(12):1009.

71. Subramanian P, Ravichandran A, Manoharan V, Muthukaruppan R, Somasundaram S, Pandi B, *et al*. Synthesis of Oldenlandia umbellata stabilized silver nanoparticles and their antioxidant effect, antibacterial activity, and bio-compatibility using human lung fibroblast cell line WI-38. Process Biochem. 2019;86:196-204.

72. Shanmugapriya K, Palanisamy S, Boomi P, Subaskumar R, Ravikumar S, Thayumanavan T. An eco-friendly Gnaphalium polycaulon mediated silver nanoparticles: Synthesis, characterization, antimicrobial, wound healing and drug release studies. J Drug Deliv Sci Technol. 2021;61:102202.

73. Oyeleke SA, Ajayi AM, Umukoro S, Aderibigbe A, Ademowo OG. Anti-inflammatory activity of Theobroma cacao L. stem bark ethanol extract and its fractions in experimental models. J Ethnopharmacol. 2018;222:239-48.

74. Yatoo M, Gopalakrishnan A, Saxena A, Parray OR, Tufani NA, Chakraborty S, *et al*. Anti-inflammatory drugs and herbs with special emphasis on herbal medicines for countering inflammatory diseases and disorders-a review. Recent Pat Inflamm Allergy Drug Discov. 2018;12(1):39-58.

75. Yuan L, Zhang F, Shen M, Jia S, Xie J. Phytosterols suppress phagocytosis and inhibit inflammatory mediators via ERK pathway on LPS-triggered inflammatory responses in RAW264. 7 macrophages and the correlation with their structure. Foods. 2019;8(11):582.

Cite this article: Dubey T, Bhanukiran K, Das K, Hemalatha S. Development and Evaluation of Bio fabricated Silver Nanoparticles from *Blumea lacera* for *In-vitro* Antibacterial, Antioxidant and Anti-inflammatory Activity. Pharmacogn J. 2023;15(2): 266-278.